Sensor applications

Influence of Position on Optoelectronic Strain Measurement Systems for Flywheels

Matthias Rath, Bernhard Schweighofer, and Hannes Wegleiter

Christian Doppler Laboratory for Measurement Systems for Harsh Operating Conditions, Institute of Electrical Measurement, Sensor Systems, Graz University of Technology, 8010 Graz, Austria

Manuscript received 12 July 2023; accepted 15 July 2023. Date of publication 1 August 2023; date of current version 23 August 2023.

Abstract—The main component of flywheel energy storage systems (FESS) is the flywheel rotor itself: a rotating mass which stores kinetic energy. Ongoing research in the field of FESS requires constant condition monitoring of the flywheel rotor, especially when new composite materials and flywheel rotor manufacturing methods are investigated. Optoelectronic strain measurement (OESM) is a method to contactlessly measure the flywheel rotor's radial deformation as well as its position in the radial plane via a special reflective pattern on the flywheel which is read via optical sensors. This letter presents a simulation model to estimate the influence of pattern offset and in-plane movement of the flywheel on an array of multiple sensors. The measurement values from multiple sensors can be fused to mitigate the influence of cross sensitivity between flywheel deformation and position measurements. The influence of out-of-plane movement on the measured values is evaluated via measurements on a test bench setup, where the sensor distance can be controlled by a stepper motor.

Index Terms—Sensor applications, flywheel, strain measurement, uncertainty.

I. INTRODUCTION

Flywheel energy storage systems (FESS) are electromechanical systems that convert electrical energy into kinetic energy which is stored in the momentum of the rotating mass [1]. The key components of the FESS are the flywheel rotor itself and the electric machine which can operate as either a motor to accelerate the flywheel and store energy or as a generator to decelerate the flywheel and recuperate electric energy. Other important components are the bearing system, safety and vacuum housing, vacuum pumps, cooling system, and sensors for monitoring all these components. FESS can be deployed in specific use cases that require fast responding, short-term energy storage with a large cycle count like for grid stabilization [2], [3].

The energy an FESS can store increases with the flywheel's rotation speed which requires materials with high tensile strength to withstand the rotational forces. Carbon-fiber-reinforced polymer (CFRP) is a material with great potential but has special demands on manufacturing [4], [5]. Monitoring the condition of the CFRP parts of a composite flywheel is of special interest for further research in high-energy-density FESS.

In the scope of this letter, we will only focus on monitoring the radial strain and position of the flywheel rotor via optoelectronic strain measurement (OESM), a contactless monitoring method [6], [7]. Contactless methods have advantages over competing methods like strain gauges in that no electronic components have to be installed on the rotating flywheel and that the measurement signals do not have to be transmitted from the rotating flywheel to the stationary part of the FESS [8], [9]. Since slip rings tend to overheat at the target speeds of up to 30 kr/min, wireless data transmission would require at least some basic circuitry on the flywheel, while OESM only requires a treatment of the surface to apply a special reflective pattern.

Corresponding author: Matthias Rath (e-mail: matthias.rath@tugraz.at).
Associate Editor: J. M Corres.
Digital Object Identifier 10.1109/LSENS.2023.3300811

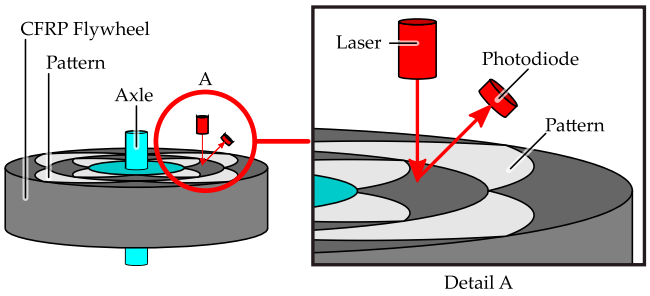

Fig. 1. Basic operation of an optoelectronic strain measurement system on a flywheel [12].

Measuring the strain of a flywheel using optical methods is a well-known procedure [6], [10]. What is missing in these publications, however, is an analysis of the extent to which the movement of the flywheel in the axial or radial direction affects these measurement methods. Therefore, the aim of this work is the investigation of these effects using a 2-D MATLAB simulation model as well as an experimental flywheel test bench. The influences of the optical parameters of the OESM sensor have been investigated in previous papers [11], [12].

The next section will introduce the basic operation principle on OESM systems as well as the influences on the measurement, which are investigated in this letter.

II. OPTOELECTRONIC STRAIN MEASUREMENT BASICS

The basic principle of optoelectronic strain measurement on a flywheel rotor is shown in Fig. 1. A special pattern is applied to the top circular surface of the cylindrical flywheel rotor. The pattern consists of multiple reflective and nonreflective petal-like shapes whose edges are spiral segments. An example of the petal-like pattern is shown

This work is licensed under a Creative Commons Attribution 4.0 License. For more information, see https://creativecommons.org/licenses/by/4.0/

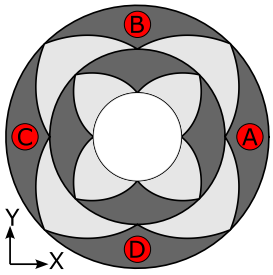

Fig. 2. Reflective spiral pattern and sensor positions A, B, C, and D [11].

in Fig. 2. The pattern has an optical contrast to the flywheel surface material. For steel flywheels which are reflective, the pattern is applied with black spray paint. For CFRP flywheels which are naturally black, the pattern is applied with a reflective paint. When the flywheel deforms due to rotational forces, the pattern deforms together with the flywheel. Stationary optical sensors consisting of a laser light source and a photodiode scan the pattern when the flywheel is in rotation. Because of the difference in reflectivity between the pattern and the flywheel surface, the sensor sees a series of dark and light pulses. Due to the spiral form of the contrasting edges of the pattern, the pulse width corresponds to the relative radial shift between sensor and pattern. A series of sensors in different positions is utilized, as shown in Fig. 2. This allows a distinction between a shift caused by flywheel deformation (usually radial stretching of the flywheel) and a shift caused by flywheel in-plane movement (movement in the radial plane).

The flywheel deformation and movement in the X-direction for the four-sensor setup shown in Fig. 2 can be expressed as

$$d_x = \frac{s_A + s_C}{2} \tag{1}$$

$$p_x = \frac{s_A - s_C}{2} \tag{2}$$

where d_x is the deformation (stretching), and p_x the position of the flywheel in the X-direction. The calculation for the Y-direction can be done in the same way with shift values of sensors B and D. The individual shift between pattern and sensor is denoted as s, where the subscript corresponds to the sensor. The shift can be considered the raw sensor value which is calculated from the measures of the pulse width and a pattern specific scaling factor [6], [11]. The shift a single sensor measures can either be caused by a flywheel deformation or by position movement and a distinction is only possible when evaluating the measurements of multiple sensors. We use a setup with four sensors shown in Fig. 2, where a pair of sensors each is responsible for measurements in one cardinal direction X and Y. This letter describes simulation and results of the influence that flywheel movement and pattern offset in Y-direction exert on the deformation and position measurement.

III. SIMULATION SETUP FOR IN-PLANE MOVEMENT AND PATTERN OFFSET

The influence of in-plane flywheel movement as well as in-plane pattern offset on the deformation and displacement calculation are investigated in a simulation study. In-plane movement can be caused by resonant vibrations in the flywheel when the bearings are elastically mounted, or through external forces when the flywheel is used in

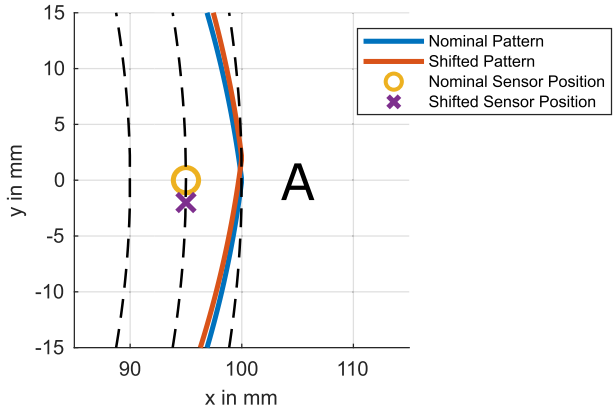

Fig. 3. Detail view of the simulation model for sensor position A. Example of the shifted pattern and sensor position compared to the nominal position.

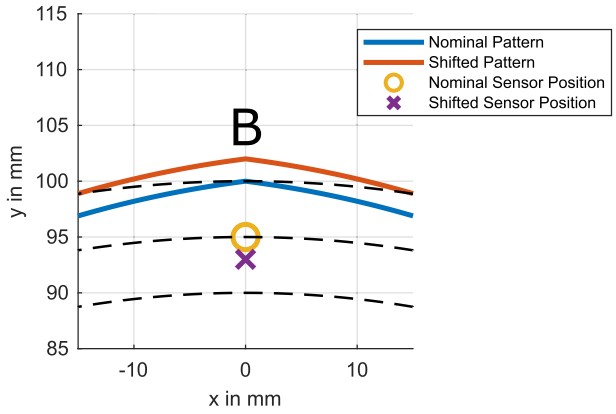

Fig. 4. Detail view of the simulation model for sensor position B. Example of the shifted pattern and sensor position compared to the nominal position.

a nonstationary application like in vehicles [13], [14]. Because the flywheel, pattern, and center of rotation move as a whole relative to the four sensors, this scenario is simulated shifting all of the sensors in the negative Y-direction. Movement of the sensors as a group and also relative to each other is also possible in an FESS through vibrations, but they are considered to be much smaller than the movement of the flywheel itself and therefore neglected. A pattern offset can occur because of alignment inaccuracies when applying the pattern via a stencil and spray paint. The pattern is offset in relation to the center of rotation which is simulated by shifting the pattern in the positive Y-direction while keeping the center of rotation constant.

Because of the symmetric sensor setup, we only need to apply a sensor and a pattern shift in the Y-direction for the investigation of their influences. An example of the nominal pattern and sensor position versus their shifted versions can be seen in Figs. 3 and 4. The simulation is parametrized for a small test bench rotor with a 100-mm radius, where each ring of the OESM pattern stretches radially over 10 mm. The nominal sensor radius is at 95 mm, placing the sensors right in the middle of a pattern ring.

Radial sensor position also influences the measurements but to a lesser extent. For the scope of this letter, only one fixed radial sensor location is investigated. The radial position was chosen as close as possible to the point of maximum radial deformation.

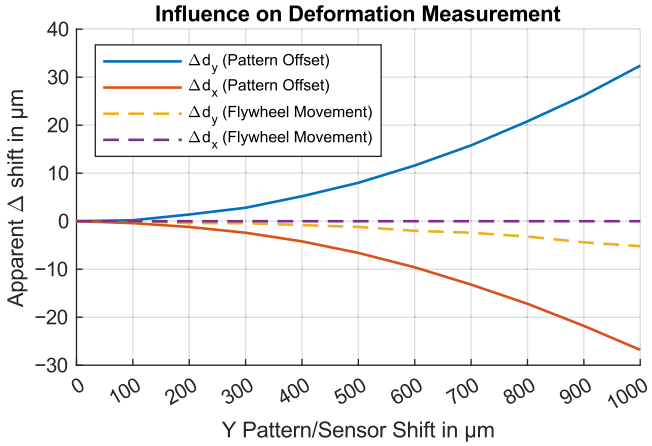

Fig. 5. Influence of pattern offset and flywheel movement in the *Y*-direction on the deformation measurement d. Δd denotes the change compared to the initial value in the direction of the subscript.

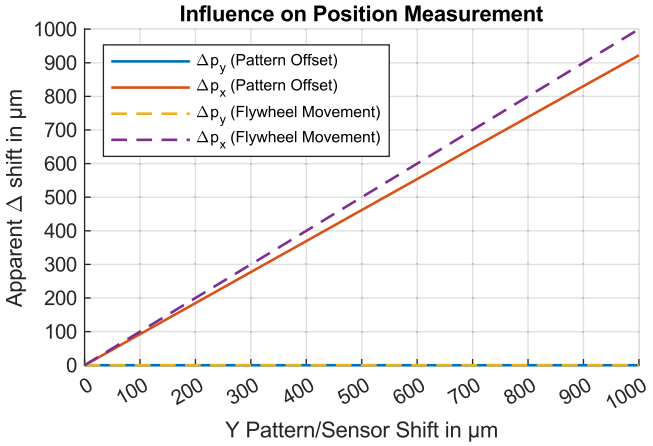

Fig. 6. Influence of pattern offset and flywheel movement in *Y*-direction on the flywheel position measurement m. Δd denotes the change compared to the initial value in the direction of the subscript.

IV. MEASUREMENT SETUP FOR OUT-OF-PLANE MOVEMENT

The influence of the out-of-plane movement (in axial direction) is investigated experimentally via measurements on a test bench. A steel flywheel is equipped with a single OESM sensor configured for a nominal distance to the flywheel surface of 8 mm. The pattern is applied to the flywheel with black spray paint and a stencil cut from vinyl foil. To measure the influence of different sensor distances, the OESM sensor is mounted on a stepper-motor-controlled platform. For the experiment, the flywheel is spun at a fixed speed of 40 Hz and the photodiode voltage signal is recorded with a Picoscope 4444 USB oscilloscope. In addition, a Keyence IL-65 CMOS laser distance sensor is used to measure the movement of the flywheel relative to its housing.

V. RESULTS

A. Simulation of In-Plane-Movement

The influence of pattern offset is simulated for values of up to 1 mm which is realistic for manual pattern application. Flywheel movement on a test bench was observed to be lower than 200 μm but can depend on the actual design of the elastic bearing mounting system. Because elastically mounted flywheels are able to move in radial direction, the influence on the statically mounted sensor array is of interest. Influence of movement is also simulated for values of up to 1 mm to account for that.

Fig. 5 shows the results of the simulation for deformation calculation. A pattern offset in *Y*-direction influences the deformation calculation in the direction of the offset (sensors BD) as well as the perpendicular direction (sensors AC). Flywheel movement in the *Y*-direction on the other hand is naturally compensated for in the direction of the movement (sensors BD) but influences the measurement in the perpendicular direction (sensors AC).

Fig. 6 shows the results of the simulation for position calculation. A movement in the *Y*-direction actually is the position change we want to measure, so it directly corresponds with the position calculation for sensors BD. The influence of *Y*-movement on the perpendicular set of sensors (AC) is naturally compensated for. A pattern *Y*-offset in the sensor direction (BD) results in a nearly direct influence on the calculated position while the influence on the perpendicular sensors (AC) again is compensated for.

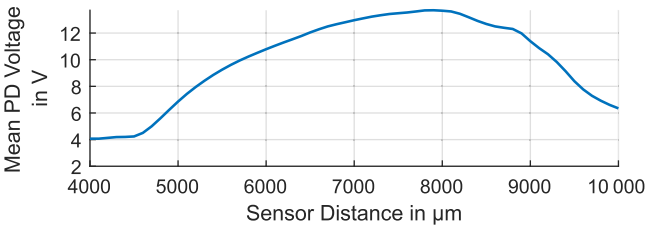

Fig. 7. Influence of the sensor distance on the intensity of the photodiode (PD) signal over the high time of the signal.

In conclusion, the influence of the pattern offset cannot be neglected and calibration and compensation schemes are required.

B. Measurement of Out-of-Plane Movement

The influence of the sensor distance to the flywheel surface is investigated experimentally and the following section presents the findings.

At the nominal sensor distance, the maximum intensity of the reflected light from the pattern is reflected back to the photo diode. Changes in sensor distance influence the amount of light hitting the OESM sensor's photodiode. As a measure of light intensity, the photodiode signal is averaged over only the high-time parts of the pulse signal which correspond to the reflective patches of the pattern. The low-time pulses would correspond to the dark patches of the pattern. The resulting curve in Fig. 7 shows a very distinctive change in light intensity depending on the sensor distance. The sensor was designed for a nominal distance of 8 mm, which is the distance of maximum light intensity. When the relation between distance and light intensity is known, the OESM sensor can (within limits) also be used to measure the out-of-plane movement of the flywheel (in axial direction). A limiting factor is the inhomogeneity of the reflective surface coating, which itself also leads to changes in light intensity.

The nonlinear behavior is due to the change in area where the reflected laser spot overlaps with the photodiode. At extreme distances, the 3-D-printed sensor enclosure can cause occlusion of the reflected light.

Converting the photodiode signal's pulses into an apparent shift gives us the influence of the out-of-plane movement on the calculated flywheel movement and position. The results are shown in Fig. 8, where the influence over a wide range of sensor distances can be considered

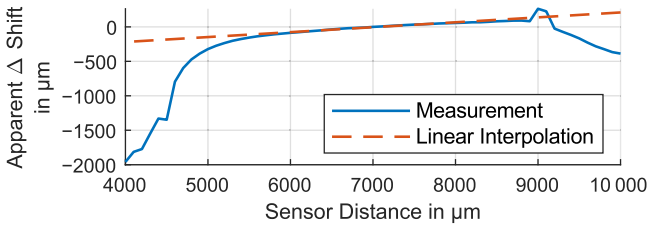

Fig. 8. Influence of the sensor distance on the measurement of the measured radial shift between sensor and flywheel.

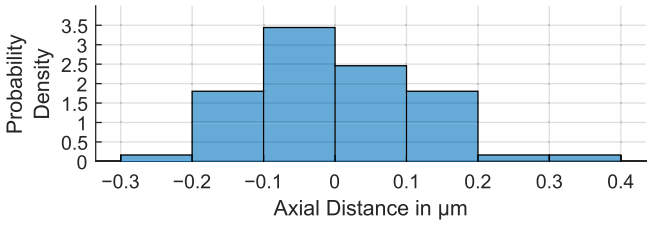

Fig. 9. Histogram of the measured axial flywheel movement relative to its housing. Normalized as a probability density function.

as linear with a slope of 71 μm/mm (linear interpolation in the sensor distance range 6–8 mm).

The measured out-of-plane movement for the test bench flywheel at a static speed of 40 Hz is shown as a probability distribution in Fig. 9. Out-of-plane movement was below 1 μm, which results in a negligible influence on the apparent shift.

VI. CONCLUSION

This letter was conducted to gain insight into the modes and relative importance of movement and pattern alignment issues on an OESM system. The need for a calibration scheme to reduce the influence of pattern offset was identified. It could be shown in test bench measurements that the measured light intensity correlates with the sensor distance, which might provide an OESM system with additional distance measuring capabilities. The developed 2-D MATLAB simulation model can be parametrized for different flywheel and pattern sizes for application on a full-sized FESS.

ACKNOWLEDGMENT

This work was supported in part by the Austrian Federal Ministry for Digital and Economic Affairs, in part by the National Foundation for Research, Technology and Development, in part by the Christian Doppler Research Association, and in part by the TU Graz Open Access Publishing Fund, Austria.

REFERENCES

[1] G. Genta, *Kinetic Energy Storage—Theory and Practice of Advanced Flywheel Systems*. Oxford, U.K.: Butterworth-Heinemann, 1985.

[2] A. Buchroithner et al., "Grid load mitigation in EV fast charging stations through integration of a high-performance flywheel energy storage system with CFRP rotor," in *Proc. IEEE Green Energy Smart Syst. Conf.*, 2021, pp. 1–8.

[3] D. Rekioua, "Energy storage systems for photovoltaic and wind systems: A review," *Energies*, vol. 16, no. 9, 2023, Art. no. 3893.

[4] R. Emerson and C. Bakis, "Relaxation of press-fit interference pressure in composite flywheel assemblies," in *Proc. Int. SAMPE Symp. Exhib.*, 1998, pp. 1904–1915.

[5] S. K. Ha, H. H. Han, and Y. H. Han, "Design and manufacture of a composite flywheel press-fit multi-rim rotor," *J. Reinforced Plastics Composites*, vol. 27, no. 9, pp. 953–965, 2008.

[6] R. P. Emerson and C. E. Bakis, "Optoelectronic strain measurement for flywheels," *Exp. Mechanics*, vol. 42, no. 3, pp. 237–246, 2002.

[7] M. Jolly et al., "Review of non-destructive testing (NDT) techniques and their applicability to thick walled composites," *Procedia CIRP*, vol. 38, pp. 129–136, 2015.

[8] A. K. A. Kroworz, "Non-destructive testing of structures using optical and other methods: A review," *Struct. Durability Health Monit.*, vol. 12, no. 1, pp. 1–18, 2018.

[9] B. Karaş, V. Beedasy, Z. Leong, N. A. Morley, K. Mumtaz, and P. J. Smith, "Integrated fabrication of novel inkjet-printed silver nanoparticle sensors on carbon fiber reinforced nylon composites," *Micromachines*, vol. 12, no. 10, 2021, Art. no. 1185.

[10] M. L. Simpson and D. E. Welch, "Optoelectronic-strain-measurement system for rotating disks," *Exp. Mechanics*, vol. 27, no. 1, pp. 37–43, 1987.

[11] M. Rath, R. Preßmair, B. Schweighofer, and G. Brasseur, "Feasibility evaluation of optoelectronic strain measurement for flywheel rotors," in *Proc. IEEE Int. Instrum. Meas. Technol. Conf.*, 2020, pp. 1–6.

[12] M. F. Rath, B. Schweighofer, and H. Wegleiter, "Uncertainty analysis of an optoelectronic strain measurement system for flywheel rotors," *Sensors*, vol. 21, no. 24, 2021, Art. no. 8393.

[13] W. Zhang and J. Yu, "Modeling of vehicle-mounted flywheel battery considering automobile suspension and pulse road excitation," *Energies*, vol. 16, no. 11, 2023, Art. no. 4288.

[14] P. Ji, W.-W. Nie, and J.-L. Liu, "Research on magnetic coupling flywheel energy storage device for vehicles," *Appl. Sci.*, vol. 13, no. 10, 2023, Art. no. 6036.